Natural Hazards (2024) 120:7195–7209
https://doi.org/10.1007/s11069-024-06508-1

ORIGINAL PAPER

Maximum wind speed radius and filling model of tropical cyclones in the coastal regions of Southeast China

Yong Quan[1] · Chao Tan[1] · Baoshan Chen[1]

Received: 21 September 2023 / Accepted: 14 February 2024 / Published online: 10 March 2024

Abstract

The estimation of extreme wind speed for tropical cyclones (TCs) is often achieved through Monte Carlo numerical simulation method. The accuracy of the Monte Carlo simulations is directly affected by the extent to which the probability distributions and correlations of wind field parameters can be determined correctly. In order to enrich the information on key TC parameters in the coastal areas of southeast China, based on the analysis of historical data of TCs and near-ground measured data by meteorological departments, the function relationships between statistical values of the maximum wind speed radius and the central pressure difference are explored at first in the present study. Secondly, the coastal areas of southeast China are subdivided into four regions according to the influence factors of TC parameters and a new filling model for post-landfall TCs is also proposed for these regions. Finally, the accuracy and effectiveness of the proposed function relationships and the filling model are validated through a comparison of the present predicted results with those of previous methods and measured results.

Keywords Tropical cyclone · Wind field model · China

1 Introduction

Strong winds are a major cause of natural disasters at present. For areas prone to TCs, it is very important to determine the possible extreme wind speeds of TCs accurately to ensure the structural safety of new constructions (Simiu and Yeo 2019). Due to the scarcity of measured wind speed data, the Monte Carlo method is commonly used to perform numerical simulations of TCs based on the probability distributions and correlations of TC wind field parameters, in order to obtain the corresponding wind speed samples and predict extreme values of wind speed.

Batts et al. (1980) improved the method first proposed by Russell (1971) which simulated TCs with a random method. The resulting "Batts wind field model" is considered to be the first-generation wind field model. Vickery and Twisdale (1995) and Vickery et al.

✉ Yong Quan
quanyong@tongji.edu.cn

1 State Key Laboratory of Disaster Reduction in Civil Engineering, Tongji University, No. 1239 Siping Road, Yangpu District, P. O. Box 200092, Shanghai, People's Republic of China

(2000a) incorporated the radial pressure distribution field proposed by Holland (1980) into the models of Shapiro (1983) and Chow (1971), proposed two types of numerical solutions of TC wind fields with different precisions, and established a new filling model which is regarded as the second-generation wind field model. Vickery and Twisdale (1995) also compared the Batts model with Shapiro model and validated the latter's advantages. Vickery et al. (2000a) first proposed a new wind field model that considered the influence of sea surface roughness and the temperature difference between the air and the sea surface, and subsequently presented a model named the Full Empirical Track Model (Vickery et al. 2000b). Kepert (2001, 2010) proposed a three-dimensional wind field model, calculated and validated axisymmetric slab models and boundary layer models from the governing equations through simplified assumptions. Considering multiple coupled typhoon conditions, Fang et al. (2018a, 2018b) introduced a model incorporating variations in altitude pressure fields and roughness changes, and verified its accuracy with observed data. Fang et al. (2020) established a TC model for the northwest Pacific region and validated its applicability. Yang et al. (2021a, 2021b) successively developed parameterized models for TCs considering vertical convection processes, land cover and terrain effects.

The correlations among TC wind field parameters have always been a focus area of wind engineering research. Yasui et al. (2002) and Xiao et al. (2011) obtained the probability distributions of some TC parameters and empirical formulas indirectly by analyzing the measured data of sea level pressure at meteorological stations during the development of TCs. Based on TC data from the Bay of Bengal, Jakobsen and Madsen (2004) fitted the function relationship between the Holland parameter B and maximum wind speed (one-minute time lag) at a distance of 500 m from the TC center. Zhao et al. (2009) analyzed the sensitivity of each wind field parameter with the target of extreme wind speed. The central pressure difference Δp, Holland parameter B, and maximum wind speed radius R_m all display a strong sensitivity to the predicted values. Huang et al. (2016), Huang and Sun (2018) proposed a new method for calculating B based on TC data from Hong Kong. Fang et al. (2018a, b, c, 2019) pointed out significant differences among the key TC parameters in different regions and suggested consideration of regional characteristics to determine relevant parameters. Huang et al. (2021) proposed an overall framework for simulating the entire path of typhoons in the northwest Pacific region. Wei et al. (2023) summarized different R_m and B models in different sea areas. Based on historical best track data from the Japan Meteorological Agency (JMA), they introduced a three-dimensional wind field model and conducted random simulations for typhoons in coastal cities of China. The results showed noticeable differences of R_m and B not only among different sea areas but also within the same sea area. Thus it can be seen that there are wide variations in the results obtained from different studies and the specific forms of the correlations are still not clear. Accurate and unified conclusions about the correlations among TC wind field parameters are lacking and further researches are necessary.

The changes of central pressure difference after TCs landfall have also been studied. Batts et al. (1980) proposed a TC filling model with the time as an independent variable. However, this model only considers the influence of approach angle and TC landfall time. Schwerdt et al. (1979) analyzed sixteen hurricanes that landed in the coastal areas of the United States and subdivided these areas into three regions in accordance with the filling rate of the hurricane speeds. Ho et al. (1987) showed that the filling rate was closely related to the geographic locations of landfall and the initial intensity of TCs. Georgiou et al. (1983) established a filling model that incorporated the travel distance of TCs after landfall as an independent variable. They also subdivided the coastal areas of the United States into four regions and listed the corresponding filling formulas for each region.

Based on the regional subdivisions (Schwerdt et al. 1979), Vickery and Twsdale (1995) also established a filling model incorporating time as an independent variable and established a linear relationship between the filling-rate coefficient and the initial landfall pressure difference Δp_0. Based on Vickery model, Xiao et al. (2011) and Jin (2023) also fitted the filling model parameters corresponding to some regions along the southeast coasts of China. Although many models have been proposed, the kind of variables incorporated in these models remains relatively sparse. Therefore, a more integrated method is necessary in order to solve this problem.

Based on historical TC data obtained from meteorological departments in the coastal areas of southeast China, the present study investigates the statistical characteristics of maximum wind speed radius (R_m) and the filling issue of TC post-landfall. Firstly, the function relationships between statistical values of R_m and central pressure difference Δp are fitted. Secondly, the coastal areas of southeast China are subdivided into four regions in accordance with the influence factors and a new TC filling model is also introduced. Finally, the accuracy and effectiveness of the fitted function relationships and the new filling model are validated through a comparison of the present predicted results with those of previous models and TC measured results. The filling model parameters for four regions are also given.

The paper is structured as follows: Sect. 2 describes the data sources of TCs. Section 3 explains the methodology used in this study. The obtained results and discussion are presented in Sect. 4 while the conclusions are stated in Sect. 5.

2 Data procurement

In this study, two sets of data sources are used, corresponding to the researches of the maximum wind speed radius and the filling model of post-landfall TC, respectively.

2.1 Hong Kong observatory

Hong Kong is one of the typical developed cities in the coastal areas of southeast China. It holds a unique geographical position, adjacent to the Pearl River Delta, bordering Guangdong Province and serves as a significant center for international trade and finance. Additionally, Hong Kong features diverse topography, including mountains, hills, and plains. The main components of Hong Kong are as follows: Hong Kong Island is the main island in the region, with a high elevation and the highest point being the Victoria Peak at about 552 m above the sea level. The New Territories occupies most of the land in Hong Kong and is relatively flat, while the Kowloon Peninsula, which connects Hong Kong Island and the New Territories, is low lying. Overall, Hong Kong has a wide range of elevations, from plains to mountains, making it a representative region for this study.

In order to study R_m in the coastal areas of southeast China, TC data provided by the Hong Kong Observatory are utilized in this paper. Hong Kong Observatory has deployed numerous and high density meteorological stations in Hong Kong, including automatic weather stations, wind stations and rainfall stations, totaling around ninety stations. The study uses historical records (Tropical Cyclone Annual Publications 1971–2014) of TC tracks and wind field parameters impacting Hong Kong from 1998 to 2013, as well as synchronous measured sea-level pressure data from various meteorological stations, including the Hong Kong Observatory, Hong Kong International

Fig. 1 Location map of Hong Kong meteorological stations (Hong Kong Observatory, 2023)

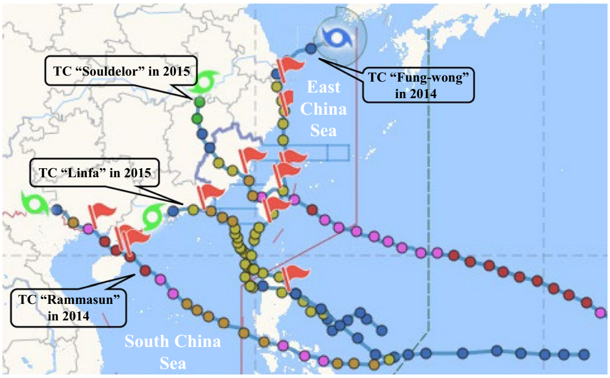

Fig. 2 Representative TCs development tracks in the coastal areas of southeast China (Fujian Provincial Department of Water Resources, 2023)

Airport, Waglan Island, Cheung Chau and others. Figure 1 illustrates the geographical distribution of regions and meteorological stations in Hong Kong.

2.2 Fujian provincial department of water resources

Historical records of the TC tracks and wind field parameters from 1985 to 2013, provided by the Fujian Provincial Department of Water Resources, are utilized to study the TC post-landfall filling rate in this study. These data included information such as the latitude and longitude of TC centers, central pressures, overall speeds, seventh-level wind circle radii and tenth-level wind circle radii. The latter two are the radius to the seventh-level and tenth-level wind speed corresponding to the Beaufort scale, respectively.

Due to the large volume of data, only four representative TCs that impacted corresponding coastal regions are selected for the subsequent validation of the filling model, which include Rammasun in 2014, Fung-Wong in 2014, Soudelor in 2015, and Linfa in 2015, respectively. Their development tracks are illustrated in Fig. 2.

3 Methodology

The first part of this study fits the function relationships between statistical values of R_m and Δp. Next, the coastal areas of southeast China are subdivided into four regions and a new filling model is also proposed corresponding to each region in the second part.

3.1 Maximum wind speed radius

Since direct measurements of R_m are not provided in the TC yearbooks, there are two primary methods available for obtaining sampled values of R_m indirectly in the current studies. The first method is based on the radial pressure distribution formula (1) proposed by Holland (1980),

$$p = p_c + \Delta p \exp\left(-\left(\frac{R_m}{r}\right)^B\right) \tag{1}$$

where p and p_c are the sea level pressure and the central pressure of a TC in hPa measured by the weather stations, respectively. r is the distance from weather stations to the TC center in km. B is the radial pressure distribution index (Holland parameter).

Yasui et al. (2002) also calculated R_m sample values based on formula (1) and found that the probability distribution functions of R_m followed a normal distribution or a lognormal distribution corresponding to different values of Δp.

The second method is based on the fitting formula (2) obtained by Li et al. (1995), using Sheets (1980) theory and sixth-level wind circle radii from measured values.

$$R_m = R_6 \left(V_6 / V_{max}\right)^k \tag{2}$$

where V_6 is the Beaufort scale corresponds to the sixth-level wind speed, which is generally 10.8 m/s and R_6 is the radius to V_6 wind speed in km (named sixth-level wind circle radii). V_{max} is the 2-min mean maximum sustained wind speed in m/s near the TC center. k varies from 1/0.5 to 1/0.7. Xiao et al. (2011) also derived a linear relationship between $\ln R_m$ and Δp based on this method.

In the present study, the historical data of TC wind fields in the Tropical Cyclone Annual Publications from 1971 to 2014 (Hong Kong Observatory 2023) and the sea level pressure values from meteorological stations are used to calculate a large number of R_m samples based on the formula (1). Subsequently, the function relationships between statistical values of R_m and Δp is also fitted.

For the issue of Holland parameter B values, various previous studies (Holland 1980, 2008; Love and Murphy 1984; Vickery et al. 2000a, b; Jakobsen and Madsen 2004) have considered B as a random variable and explored the relationships between B and other parameters. Due to the focus of this study is R_m rather than B, here we consider B as a fixed value. Holland (1980) pointed out that a reasonable range of values for B was from 1.0 to 2.5, which is widely recognized and applied in the field of wind engineering. Therefore, in the process of calculating R_m samples, a series of fixed B values ranging from 1.0 to 2.5 (with an interval of 0.1) are utilized.

Considering the possibility of atmospheric pressure changes caused by non-TC climate effects and the influence of measurement errors in the values of Δp, the method similar to

Fig. 3 Relationship between R_m and Δp

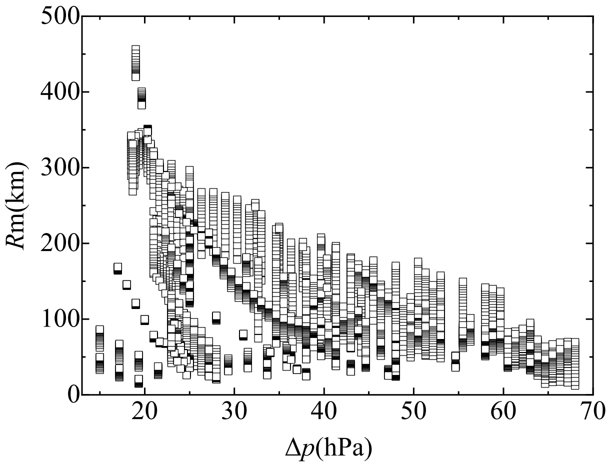

Fig. 4 The fitting relationship between mean values of R_m and Δp

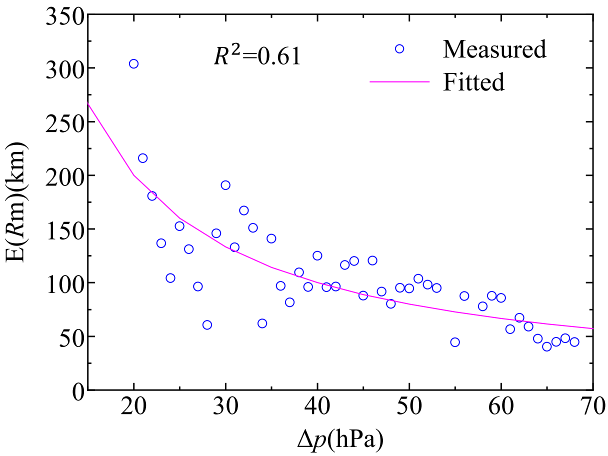

that in Yasui et al. (2002) is adopted to filter the conditional wind field parameter records in the study. The following conditions are imposed that:

(1) the values of Δp were below 990 hPa,
(2) center of the TC was 100–500 km from the meteorological stations,
(3) the sea level pressures measured by the stations were below 1000 hPa.

After the 158 TCs data that impacted Hong Kong from 1985 to 2013 are filtered and calculated, a total of 5728 sample points are obtained to study the statistical characteristics of R_m. Figure 3 illustrates the relationship between R_m and Δp for TCs. As shown in this figure, R_m values tend to increase and disperse gradually with the decrease of Δp.

According to Yasui et al. (2002), the relationships between the statistical values of R_m and Δp can be approximated by index functions. In this study, the relationships between mean and standard deviation (SD) of R_m and Δp are fitted as fomulas (3) and (4). Figures 4 and 5 show the fitting curves to express the relationship between and the mean values of

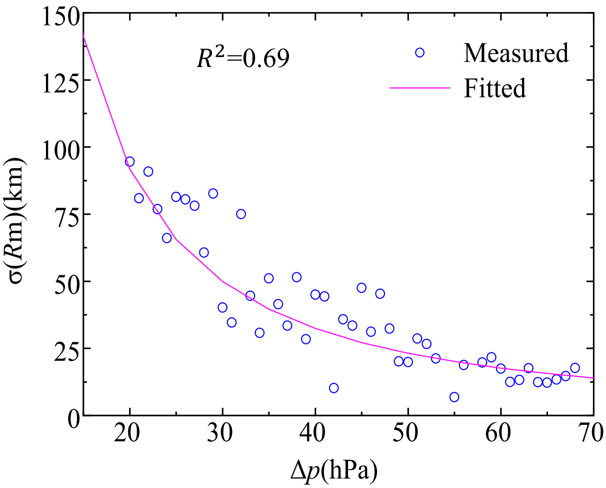

Fig. 5 The fitting relationship between standard deviations of R_m and Δp

R_m and Δp, and the relationship between SDs of R_m and Δp for TCs, respectively. Both of the curves closely express the variation of R_m with Δp and exhibit a gradual decrease with the increasing Δp. The fitting relationships are determined as,

$$\overline{R}_m = 4000/\Delta p \tag{3}$$

$$\sigma_{R_m} = 8200\Delta p^{-3/2} \tag{4}$$

The R^2 (goodness-of-fit coefficient) values for the two fitted curves are 0.61 and 0.69, respectively. It can be consider that the curves have a good fit and can accurately reflect the relationships between the statistical characteristics of R_m and Δp in the coastal areas of southeast China.

3.2 The filling model

The intensity of a post-landfall TC will decay gradually due to the cut-off of thermal energy drawn from the ocean and the energy loss caused by land friction, which can lead to a decrease in the wind speed and even a change in the wind profile. The majority of previous studies (Batts et al. 1980; Georgiou et al. 1983; Vickery and Twisdale 1995; Wang et al. 2007) found that the filling rate associated with a TC after landfall was closely related to the cyclone itself, landfall area, initial landfall intensity, and landfall approach angle, among other factors. At present, the filling of post-landfall TC intensity is mainly described by the change of the central pressure difference Δp. Xiao et al. (2011) obtained the filling rate by the ratio of Δp at any time after landfall to Δp_0 at the initial landfall time ($\Delta p/\Delta p_0$) and established a corresponding filling model to predict the changes of Δp after landfall.

In recent years of studies, the filling models were predominantly established using either the time (Batts et al. 1980; Vickery and Twisdale 1995; Xiao et al. 2011) or the travel distance (Georgiou et al. 1983) after landfall as the independent variable for different regions. However, most of these models consider the effects of only a few variables and can not reflect the influence of multiple factors on the filling issue of post-landfall TCs. Consequently, this study considers the effects of initial landfall intensity, approach angle and travel distance on the filling rate meanwhile and proposes a new filling model expressed by the following equations,

$$\Delta p(d) = \Delta p_0 e^{-ad} \tag{5}$$

$$a = a_0 + a_1 \Delta p_0 + a_2 \sin\theta + \varepsilon \tag{6}$$

where $\Delta p(d)$ and Δp_0 are, respectively, the central pressure difference when the TC has traveled a distance d (in km) after landfall in hPa, and the central pressure difference at the time of landfall in hPa. a is the filling-rate coefficient. θ is the approach angle between the TC landfall direction and the coastline of the landfall area. a_0, a_1 and a_2 are the linear regression parameters. ε is the random error term, which follows a normal distribution with a mean and SD of 0 and σ_ε, respectively.

For the convenience of analyzing, Wang et al. (2007) divided Chinese coastal areas into three zones of latitude (21–28°N, 28–35°N and 35–42°N) and conducted a statistical analysis of the landfall frequencies, durations, filling rates and other characteristics of TCs. They discovered that the filling rate varied significantly as a function of factors such as latitude, regional topography, water vapor supply in the underlying layer and environmental flow fields. However, only the statistical quantities of TC landfalls are analyzed and how various factors influences the filling rate of TCs can not be explained in their method.

In order to consider the influence of factors such as the latitude, topography and landfall frequency on TC parameters in detail, the coastal areas of southeastern China are subdivided into four geographic regions in the present study: the coastal areas near the Leizhou Peninsula (I), the coastal areas near the Pearl River Delta (II), the coastal areas of Fujian (III) and the coastal areas of Zhejiang (IV), as shown in Fig. 6. Each of their main characteristics are as follows:

The coastal areas near the Leizhou Peninsula (I) has a generally flat terrain and a tropical monsoon climate. Geographically, its southern part is adjacent to Hainan Island, exerting a certain filling effect on TCs landfall, and southwest direction faces the Beibu Gulf, resulting in the water vapor supply of the underlying layer not being completely blocked when TCs landfall from westward. The coastal areas near the Pearl River Delta (II) has a complex terrain, including hills, plateaus and mountains, and features a South Asian tropical maritime climate. The presence of a composite delta formed by the accumulation of sediment brought by the Pearl River and its tributaries in the estuarine bay makes this region unique. The coastal areas of Fujian (III) and Zhejiang (IV) are mainly influenced by the Wuyi Mountains, resulting in a larger boundary layer friction. The TCs will also be weaken when making landfall from the direction of Taiwan Island. Overall, the coastal areas near the Pearl River Delta (II) and the coastal areas of Fujian (III) have the highest frequency of TC landings.

4 Results and discussion

4.1 Validation of R_m model

In order to verify the accurancy of R_m model, measured data of TC Chan-hom (2015), a representative TC in the coastal areas of southeast China, are used for comparison. Chan-hom formed in the western North Pacific on June 30, 2015 and gradually moved northwestward. It passed through the Ryukyu Islands on July 10, intensifying into a super typhoon

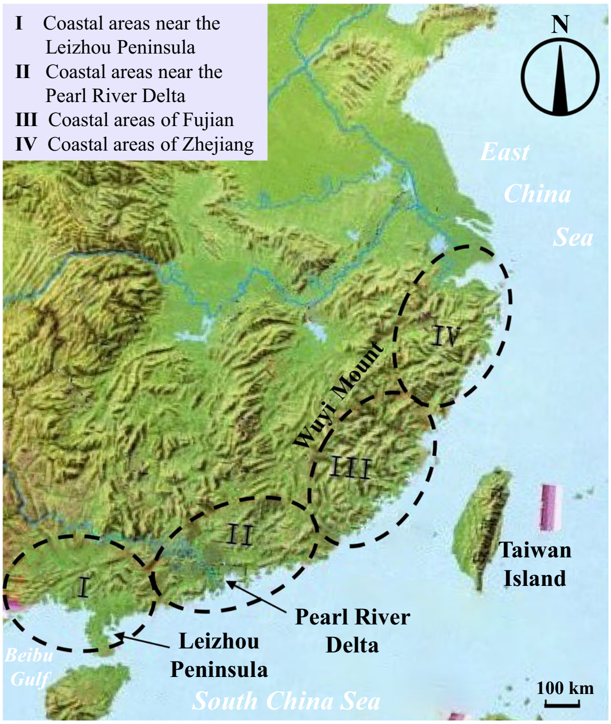

Fig. 6 Subdivision of TC landfall regions along coastal areas of southeast China

and reaching its peak intensity with an estimated maximum wind speed near 195 km/h. Then it continued to move to north and eventually transitioned into an extratropical cyclone near the western coasts of the Korean Peninsula on July 12. According to incomplete statistics, 3.528 million people in eastern China were affected, 272.9 thousand hectares agricultural areas were damaged and over 1100 houses collapsed.

Based on the method of Li et al. (1995), the R_m values calculated with the seven-level wind circle radius of Chan-hom are used as the measured reference values to compare and validate the accuracy of the fitted relationships. Figure 7 reflects the development

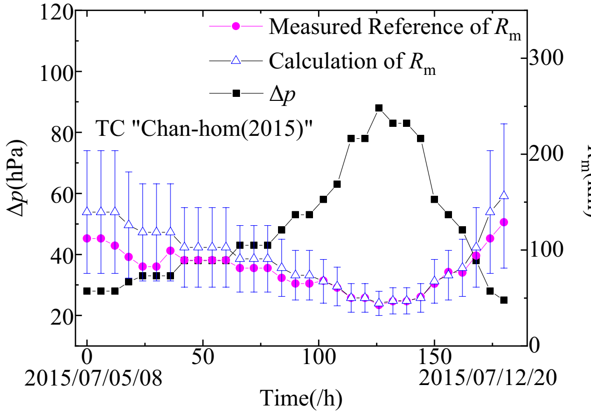

Fig. 7 TC Chan-hom in 2015

of Chan-hom over time, including Δp values, calculated R_m values by this study and measured reference R_m values. It shows the same tendency that the central pressure difference Δp increases gradually with a decrease of maximum wind speed radius R_m. During the process of TC development, the variation range of R_m calculated with proposed method envelopes measured reference R_m values well. The mean values of R_m calculated in this study are in good agreement with the measured reference R_m values for large values of Δp. Besides, the calculation error decreases with a increasing Δp.

Figure 8 presents a comparison of calculated R_m values for different Δp obtainted by the present study with those of previous models (Yasui et al. 2002; Xiao et al. 2011) and the measured reference R_m values of Chan-hom. As shown in it, the calculated R_m values by this study and Xiao model envelopes the measured reference R_m values well within the range from 20 to 40 hPa of Δp. Overall, the calculated R_m values adopted in this study can reflect the measured reference R_m values more accurately within the range from 45 to 90 hPa of Δp and the results caculated by Yasui model are relatively larger compared with the measured reference R_m values.

4.2 Parameters and validation of the filling model

In accordance with the above subdivisions of TC landfall regions for coastal areas of southeast China, a statistical analysis of the historical TC landfalls in each area is conducted and the corresponding filling model parameters are fitted and listed in Table 1, where R^2 is the multivariate determination coefficient (goodness-of-fit coefficient). There are fourteen TCs measured data in the coastal areas near the Leizhou Peninsula (I), fourteen TCs the coastal areas near the Pearl River Delta (II), seventeen TCs in the coastal areas of Fujian (III) and eleven TCs in the coastal areas of Zhejiang (IV) used during the process of calculation and fitting. Figure 9 illustrates the fitted effects of corresponding filling models using historical TC data for each region are with a type of scatter graph. The overall fitted effect is relatively poor in the coastal areas of Fujian due to the inherent bias of the statistical data.

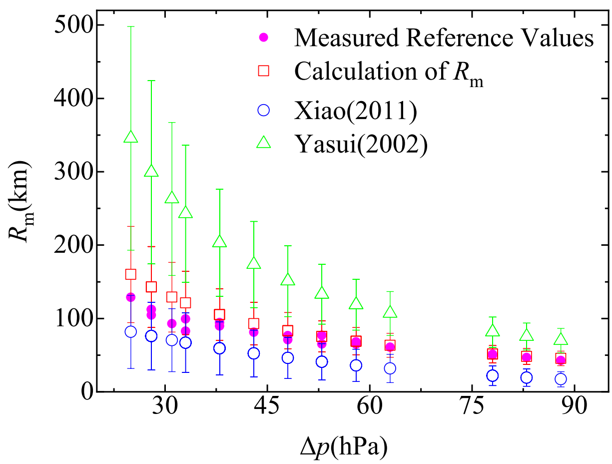

Fig. 8 Comparison of the calculation results of the various empirical models for R_m

Table 1 Parameters of filling models in various regions

Geographic areas	TC count	a_0	a_1	a_2	σ_ε	R^2
Coastal areas near the Leizhou Peninsula	14	1.70e−3	1.42e−5	6.07e−4	5.34e−4	0.18
Coastal areas near the Pearl River Delta	14	1.20e−3	2.39e−5	1.10e−3	4.81e−4	0.30
Coastal areas of Fujian	17	1.30e−3	3.54e−5	9.72e−4	1.20e−3	0.16
Coastal areas of Zhejiang	11	1.20e−3	1.86e−5	6.55e−4	3.81e−4	0.44

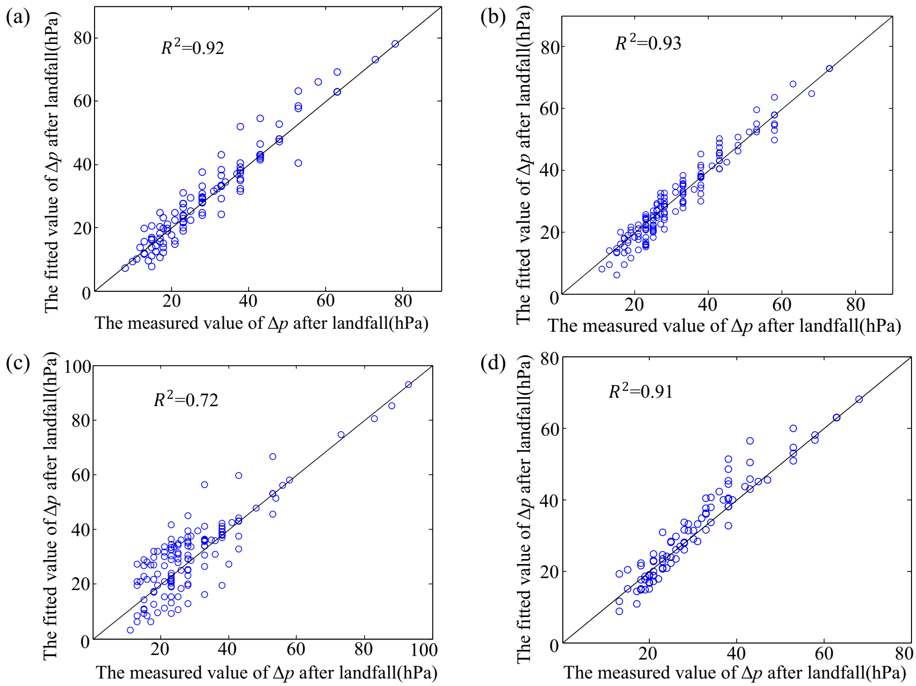

Fig. 9 Comparison of Δ*p* after landfall of historical TCs between the measured and fitted values through a scatter graph for **a** Coastal areas near the Leizhou Peninsula, **b** Coastal areas near the Pearl River Delta, **c** Coastal areas of Fujian and **d** Coastal areas of Zhejiang from 1985 to 2013

In order to compare and validate the filling model corresponding to the four regions, representative TCs are selected that made landfall in each of the four regions from 2014 to 2015, whose basic information are shown in Table 2.

Rammasun (2014) made landfall in region I on July 18, 2014 and dissipated on July 20, 2014. It caused severe disasters in China, Philippines and other areas with a total of at least 225 deaths and 8.08 billion dollars economic losses. Linfa (2015) made landfall in region II on July 9, 2015 and dissipated on July 10, 2015. It affected 2.118 million people in Guangdong Province and caused direct economic losses of 1.586 billion yuan. Soudelor (2015) made landfall in region III on August 8, 2015 and dissipated on August 10, 2015. It caused severe disasters in southeastern China and other areas, resulting in at least 59 deaths and 4.09 billion dollars economic losses. Fung-Wong (2014) made

Table 2 Basic information of four representative TCs corresponding to each region

Area	TC	Landfall	Dissipation	Category	Intensity(m/s)	Δp(hPa)
I	Rammasun	2014.07.18	2014.07.20	17	60	910
II	Linfa	2015.07.09	2015.07.10	12	35	970
III	Soudelor	2015.08.08	2015.08.10	13	38	970
IV	Fung-wong	2014.09.22	2014.09.24	10	28	985

landfall in region IV on September 22, 2014 and dissipated on September 24, 2014. It caused at least 7 deaths, 6 injuries and affected over 500,000 people.

Figure 10 shows the comparison of prediction results calculated by this study with those of previous models (Batts and Xiao model) and the measured values of the four TCs. Because of the existence of the random error term in the filling model, the Δp values used by Xiao model and this study model are the average values of 1000 simulations.

As illustrated in Fig. 10, for TC Rammasun (2014), which made landfall in the coastal areas near the Leizhou Peninsula (I), the predicted Δp values calculated with the model proposed by this study (New model) and Xiao model are closer to the measured values, whereas the predicted values generated by the Batts model are larger relatively. For TC Linfa (2015), which made landfall near the coastal areas of the Pearl River Delta (II), the predicted Δp values for the filling model proposed in this study are closer to the measured values than the predictions of other models, and the results are slightly larger than the measured values. For the TC Soudelor (2015), which made landfall in the coastal areas of

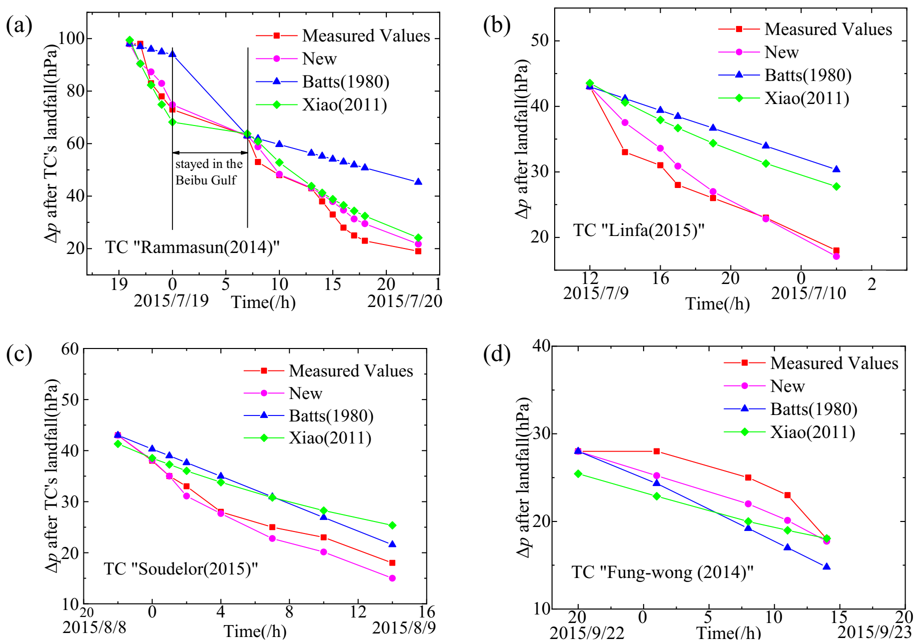

Fig. 10 Comparison of prediction results of filling model in **a** Coastal areas near the Leizhou Peninsula, **b** Coastal areas near the Pearl River Delta, **c** Coastal areas of Fujian and **d** Coastal areas of Zhejiang

Fujian Province (III), the predicted Δp values calculated with the new model conform to the measured results more accurately in the first half of the TC post-landfall travel while they are relatively smaller in the second half. The predicted Δp values of Batts model and Xiao model are both larger than the measured values during the entire period of TC post-landfall. For the TC Fung-wong (2014), which made landfall in the coastal areas of Zhejiang Province (IV), the Δp values predicted with the new filling model are closer to the measured values than the predicted values generated by other models. Moreover, since Fung-wong travelled almost parallel to the coastline along the coastal areas of Zhejiang Province in a brief period, which led to only a slight filling, the predicted Δp values of all three models are all small entirely.

In conclusion, the new filling model proposed in this study can predict the change of central pressure difference after TCs landfall in coastal regions of southeast China more accurately than the previous methods.

5 Conclusion

The statistical characteristics of tropical cyclone (TC) wind field parameters and the filling issue of post-landfall TCs in coastal regions of southeast China are analyzed in the present study. The function relationships between the statistical values of maximum wind speed radius R_m of TCs and their central pressure differences Δp are obtained through a fitting process based on historical data provided by meteorological departments. A new TC filling model is proposed and the corresponding parameters for four regions also given. The following conclusions are drawn:

(1) The mean and standard deviation (SD) values of maximum wind speed radius R_m of TCs in the coastal regions of southeast China decreases gradually with the increase of central pressure difference Δp. These relationships can be described by fitting formulas (3) and (4).

(2) The measured reference R_m values and calculated values by the proposed method show that mean values of the calculated R_m can be predicted well with large values of Δp. The results adopted in this study can reflect the measured reference R_m values more accurately than those of previous methods.

(3) The coastal areas of southeast China are subdivided into four regions according to factors such as latitude, topography, and landfall frequency that affect TC parameters. A new filling model is proposed, which can describe the filling law of post-landfall TCs more accurately.

(4) The case study results for TCs Fung-wong (2014), Rammasun (2014), Linfa (2015) and Soudelor (2015) all indicate that the values predicted with the proposed model are closer to the measured values compared to those predicted with previous methods.

Acknowledgements The authors gratefully acknowledge the support from the National Natural Science Foundation of China (51778493).

Funding This was supported by the National Natural Science Foundation of China (51778493). National Natural Science Foundation of China,51778493,Yong Quan

Declarations

Conflict of interest The authors declare that they have no known competing financial interests or personal relationships that could have appeared to influence the work reported in this paper.

References

Batts ME, Simiu E, Russell LR (1980) Hurricane wind speeds in the United States. J Struct Div 106(10):2001–2016. https://doi.org/10.1061/JSDEAG.0005541

Chow SA (1971) Study of the Wind Field in the Planetary Boundary Layer of a Moving Tropical Cyclone. Dissertation, New York University

Fang GS, Zhao L, Liang XD, Song LL, Zhu LD, Ge YJ (2018a) Applicability analysis of typhoon field parameters in engineering model for south coastal region of China based on strong typhoon Hagupit 0814. J Build Struct 39(2):106–113. https://doi.org/10.14006/j.jzjgxb.2018.02.012

Fang GS, Zhao L, Song LL, Ge YJ (2019) Investigation of design wind environment in Shanghai using an engineering-based typhoon wind model considering correlation among field parameters. J Build Struct 40(7):13–22. https://doi.org/10.14006/j.jzjgxb.2017.0681

Fang GS, Zhao L, Cao SY, Ge YJ, Pang WC (2018b) A novel analytical model for wind field simulation under typhoon boundary layer considering multi-field correlation and height-dependency. J Wind Eng Ind Aerodyn 175:77–89. https://doi.org/10.1016/j.jweia.2018.01.019

Fang GS, Zhao L, Song LL, Liang XD, Zhu LD, Cao SY, Ge YJ (2018c) Reconstruction of radial parametric pressure field near ground surface of landing typhoons in Northwest Pacific Ocean. J Wind Eng Ind Aerodyn 183:223–234. https://doi.org/10.1016/j.jweia.2018.10.020

Fang PZ, Ye GJ, Yu H (2020) A parametric wind field model and its application in simulating historical typhoons in the western North Pacific Ocean. J Wind Eng Ind Aerodyn 199:104131. https://doi.org/10.1016/j.jweia.2020.104131

Fujian Provincial Department of Water Resources. Historical Typhoon Track Information. https://slt.fujian.gov.cn/

Georgiou PN, Davenport AG, Vickery BJ (1983) Design Wind Speeds in Regions Dominated by Tropical Cyclones. J Wind Eng Ind Aerodyn 13(1–3):139–152. https://doi.org/10.1016/0167-6105(83)90136-8

Ho FP, Su JC, Hanevich KL, Smith RJ, Richards FP (1987) Hurricane climatology for the Atlantic and Gulf Coasts of the United States. NOAA Tech. Rep. NWS 38

Holland GJ (1980) An analytic model of the wind and pressure profles in hurricanes. Mon Weather Rev 108:1212–1218. https://doi.org/10.1175/1520-0493(1980)108%3c1212:AAMOTW%3e2.0.CO;2

Holland GJ (2008) A revised hurricane pressure-wind model. Mon Weather Rev 136:3432–3445. https://doi.org/10.1175/2008MWR2395.1

Hong Kong Observatory. Tropical Cyclone Annual Publications. Hong Kong: Hong Kong Observatory, 1971–2014

Hong Kong Observatory. Weather Station. https://www.hko.gov.hk/en/cis/popup.htm

Huang MF, Wang Q, Li Q, Jing RZ, Lin N, Wang LZ (2021) Typhoon wind hazard estimation by full-track simulation with various wind intensity models. J Wind Eng Ind Aerodyn 218:104792. https://doi.org/10.1016/j.jweia.2021.104792

Huang WF, Sun JP (2018) Prediction of typhoon design wind speed with cholesky decomposition method. Struct Design Tall Spec Build 27:e1480. https://doi.org/10.1002/tal.1480

Huang WF, Zhou HL, Sun JP (2016) Prediction typhoon design wind speed with empirical typhoon wind field model. J Harbin Inst Technol 02:142–146. https://doi.org/10.11918/j.issn.0367-6234.2016.02.024

Jakobsen F, Madsen H (2004) Comparison and further development of parametric tropical cyclone models for storm surge modelling. J Wind Eng Ind Aerodyn 92(5):375–391. https://doi.org/10.1016/j.jweia.2004.01.003

Jin ZM (2023) The extreme wind climate analysis of key Chinese cities. Dissertation, Tongji University

Kepert JD (2001) The dynamics of boundary layer jets within the tropical cyclone core. Part I: Linear Theory. J Atmos Sci. 58(17), 2469–2484. https://doi.org/10.1175/1520-0469(2001)058<2469:TDOBLJ>2.0.CO

Kepert JD (2010) Slab- and height-resolving models of the tropical cyclone boundary layer. Part I: Comparing the simulations. Q J R Meteorol Soc. 136(652), 1686–1699. https://doi.org/10.1002/qj.667

Li XL, Pan ZD, She J (1995) An adjustment method for typhoon parameters. J Oceanogr Huang Hai and Bo Hai Seas 13(2):11–15

Love G, Murphy K (1984) The operational analysis of tropical cyclone wind fields in the Australian northern region. Northern Territory Region Research Papers 85:44–51

Russell LR (1971) Probability distributions for hurricane effects. J Waterw, Harbors Coastal Eng. Div. 97(1), 139–154. https://doi.org/10.1061/AWHCAR.0000056

Schwerdt RW, Ho FP, Watkins RR (1979) Meteorlolgical criteria for standard project hurricane and probable maximum hurricane wind fields, Gulf of Mexico and east coast of the United States. NOAA Tech. Rep. NWS 23, U.S. Department of Commerce, Washington, DC(320)

Shapiro LJ (1983) The asymmetric boundary layer flow under a translating hurricane. J Atmos Sci 40(8):1984–1998. https://doi.org/10.1175/1520-0469(1983)040
Sheets RC (1980) Some aspects of tropical cyclone modification. Aust Meteor Mag 27:259–280
Simiu E, Yeo DH (2019) Wind Effects on Structures: Modern Structural Design for Wind, fourth edition, Wiley-Blackwell
Vickery PJ, Skerlj PF, Steckley AC, Twisdale LA (2000a) Hurricane wind field model for use in hurricane simulations. J Struct Eng 126(10):1203–1221. https://doi.org/10.1061/(ASCE)0733-9445(2000)126:10(1203)
Vickery PJ, Skerlj PF, Twisdale LA (2000b) Simulation of hurricane risk in the US using empirical track model. J Struct Eng 126(10):1222–1237. https://doi.org/10.1061/(ASCE)0733-9445(2000)126:10(1222)
Vickery PJ, Twisdale LA (1995) Wind-field and filling models for hurricane wind-speed predictions. J Struct Eng 121(11):1700–1709
Wang XF, Li HL, Wang JL (2007) Climatic features of landing tropical cyclones in China. Torrential Rain and Disasters 26(3):251–255
Wei MM, Fang GS, Zhao L, Wang ZC, Wang J, Cao SY, Ge YJ (2023) Comparative study of typhoon wind hazard estimation in coastal region of China using different wind field parameter models. J Wind Eng Ind Aerodyn 236:105398. https://doi.org/10.1016/j.jweia.2023.105398
Xiao YF, Duan ZD, Xiao YQ, Ou JP, Chang L, Li QS (2011) Typhoon wind hazard analysis for southeast China coastal regions. Struct Saf 33(4–5):286–295. https://doi.org/10.1016/j.strusafe.2011.04.003
Yang J, Chen Y, Tang YN, Yan GR, Duan ZD (2021a) A high-fidelity parametric model for tropical cyclone boundary layer wind field by considering effects of land cover and terrain. Atmos Res 260:105701. https://doi.org/10.1016/j.atmosres.2021.105701
Yang J, Chen Y, Zhou H, Duan ZD (2021b) A height-resolving tropical cyclone boundary layer model with vertical advection process. Nat Hazards 107:723–749. https://doi.org/10.1007/s11069-021-04603-1
Yasui H, Ohkuma T, Marukawa H, Katagiri J (2002) Study on evaluation time in typhoon simulation based on Monte Carlo method. J Wind Eng Ind Aerodyn 90(12–15):1529–1540. https://doi.org/10.1016/S0167-6105(02)00268-4
Zhao L, Zhu LD, Ge YJ (2009) Monte-Carlo simulation about typhoon extreme value wind characteristics in Shanghai region. Acta Aerodynamica Sinica 27(1):25–31